

Article

Determining Water Pipe Leakage Using an RP-CNN Model to Identify the Causes and Improve Poor-Accuracy Cases

Muhammad Anshari Caronge ^{1,*}, Taichi Shibuya ², Yasuhiro Arai ¹, Xinyi Dong ¹, Takaharu Kunizane ¹ and Akira Koizumi ¹

¹ Graduate School of Urban Environmental Sciences, Tokyo Metropolitan University, 1-1, Minami-Osawa, Hachioji 192-0397, Tokyo, Japan; y-arai@tmu.ac.jp (Y.A.); dong-xinyi@ed.tmu.ac.jp (X.D.); kunizane@tmu.ac.jp (T.K.); akoiz@tmu.ac.jp (A.K.)

² Faculty of Urban Environmental Sciences, Tokyo Metropolitan University, 1-1, Minami-Osawa, Hachioji 192-0397, Tokyo, Japan; ffuwa564@gmail.com

* Correspondence: ari.caronge@gmail.com

Abstract: This study aimed to assess and improve the accuracy of a water leakage detection model proposed in preliminary research. The poor results for water leakage sound (recall) and background noise (specificity) were clarified using countermeasures in accordance with each condition. Additionally, frequency amplification in the range of 500–600 Hz, the attenuation of weak components, and a band-stop filter were used to remove the 50 Hz component and harmonics. Pre-processing was carried out in the form of amplification, with weak noise removed using a band-stop filter. The results showed that the application of the proposed model improved the detection accuracy by 80% at the observation points that initially had poor accuracy. Thus, the proposed method was effective at improving the performance of the Recurrence Plot-Convolutional Neural Network (RP-CNN) model for detecting water leakages.

Keywords: convolutional neural network; noise reduction; poor-accuracy cases; principal component analysis; recurrence plot; water leakage detection



Academic Editors: Jian Kang, Olavo M. Silva and Phillip F. Joseph

Received: 11 November 2024

Revised: 11 December 2024

Accepted: 20 December 2024

Published: 3 January 2025

Citation: Caronge, M.A.; Shibuya, T.; Arai, Y.; Dong, X.; Kunizane, T.; Koizumi, A. Determining Water Pipe Leakage Using an RP-CNN Model to Identify the Causes and Improve Poor-Accuracy Cases. *Acoustics* **2025**, *7*, 2. <https://doi.org/10.3390/acoustics7010002>

Copyright: © 2025 by the authors. Licensee MDPI, Basel, Switzerland. This article is an open access article distributed under the terms and conditions of the Creative Commons Attribution (CC BY) license (<https://creativecommons.org/licenses/by/4.0/>).

1. Introduction

1.1. Background

The deteriorating state of the urban infrastructure in Japan will be costly to rectify, involving maintenance and upgrades. To address the challenges of infrastructure maintenance, renewal, and management, a national project was set up by the Council for Science, Technology, and Innovation called the Strategic Innovation Promotion Program (SIP) FY 2014–2018. As part of the SIP, the authors participated in Research and Development on Sensing Data Collection, Transmission, and Processing Technology for Social Infrastructure (Underground Structures). It was reported that the water supply pipeline network facility had a total length of 18 times the circumference of the equator, covering approximately 70% of water supply assets, worth JPY 40 trillion. As the proportion of old pipes exceeding their expected service life of 40 years increases, it will become necessary to switch from conventional methods to more advanced technologies. In order to address the issues concerning the water supply pipeline infrastructure, as part of the SIP, research was conducted on the development and placement of high-sensitivity sensor terminals in order to construct a leakage detection model based on field test data acquired in the cities of Kawasaki and Kitakyushu.

In accordance with the first stage of the SIP results, a discrimination method integrating visualization and image recognition in terms of sound data was designed. Further research was conducted on leakage discrimination based on the test data obtained in the field. A geometric visualization was performed to analyze the characteristics of leakage sounds depending on the strength of the deterministic properties. This included the use of water leakage sounds, background noise (measured when there were no leaks), and tests to determine whether the data were probabilistic [1]. Second, there was a focus on the differences in the deterministic properties of leakage sound time-series data. Additionally, the acquired data were visualized on a two-dimensional plane using a recurrence plot (RP). The visualized images served as input data for a machine learning algorithm that was used to fabricate a leakage discrimination model using a convolutional neural network (CNN) [1]. Third, an RP-CNN model was applied to the actual data to verify the accuracy of leakage discrimination. An average accuracy of more than 80% was obtained, confirming the effectiveness of the proposed combined RP-CNN method [2]. Meanwhile, the accuracy of the model was improved by applying filter processing, focusing on the frequency components of the acoustic data [3].

The results of leakage detection did not show improvements in some points, even after pre-processing. This also led to an inability to achieve a BA (balanced accuracy) exceeding 80%, which is an indicator of accuracy in machine learning [3]. In addition, points 3-B and 4-B had less accurate results, requiring additional research by five water leakage investigators (engineers with more than 10 years of experience in a water leakage detection company) using human hearing. Identifying the causes of inaccuracy at these points is a challenge that should be overcome by new technologies, the accuracy of which is superior to that achieved by conventional methods.

In this paper, Section 1 focused on the background to improving the accuracy of a previously proposed water leakage detection model [3]. This study also aimed to identify and improve causes of low accuracy. This section reviewed the latest trends in water leakage detection and highlights the originality of the present research. Section 2 described the acoustic data used during the analysis, including the items and observation equipment. This section also provided an overview of the RP-CNN model applied for water leakage detection. In Section 3, dimension reduction of acoustic data (features based on frequency components) was performed using principal component analysis (PCA). This visualizes the uniqueness of the points showing inaccuracy by positioning the samples based on the principal component scores. This section examined two types of inaccuracies—related to leakage (recall) or background noise (specificity)—including potential improvement measures for each. However, to improve recall, an amplification is specifically proposed within the frequency range of 500–600 Hz (estimated to be the characteristic range of water leakage sounds), combined with weak frequency reduction. In order to improve the specificity, the use of a band-stop filter is proposed to remove the frequency component of 50 Hz and the respective harmonics, considered AC noise (noise from the electric current source). Additionally, in this section, the pre-processing method proposed in the previous section was applied (centered on the characteristics of leakage sounds and the removal of electric current noise from the acoustic data). Leakage detection testing using the RP-CNN model was carried out, verifying the usefulness of this research. Finally, in Section 4, the conclusions were reported, along with suggestions for future work that could explore more effective ways to apply the proposed pre-processing method.

1.2. Literature Review

This section reviewed previous research on water leakage detection conducted in recent years to show the latest trends. Asada et al. [4] proposed a water leakage detection method using transient test-based techniques (TTBTs). The method uses transient phenomena in pipes depending on optimization processes and characteristics of pressure wave propagation associated with reflection to detect leakage. Furthermore, it was successfully used to detect leakage in a spiral pipe, as well as network connections with different diameters (pipe reducers). Pressure gauges were installed at pipe connection points, with operated valves at the bottom to detect leakage throughout the pipe network.

Meniconi et al. [5] used a TTBT to detect faults on long main transmission lines, which are difficult to inspect due to limited access. The analysis results indicated that this approach could reduce the adverse effects of changes in initial conditions and flow boundaries, allowing the identification of issues in the system. However, only specific areas could be thoroughly eliminated, with two leaks detected with good precision. The system's complexity, as a result of branching off the main pipeline and interactions with pressure waves during transients, complicated the implementation of TTBTs, as additional pressure waves produced by the branching must be identified [6,7]. The development of methods focusing on transient phenomena at pipe branches aims to expand leak detection to more complex systems [8–10].

Duan [11] investigated the effect of pipe joints on transient frequency response using numerical simulations in the frequency and time domains and the linear transfer matrix method. The results indicated that this method is more effective for detecting pipe leaks than measuring leaks. Kim et al. [12] and Kim [13] also conducted experiments on transient-based leak detection for multi-branch pipes.

Shirahata and Numazu [14] conducted research using several ensemble learning methods, including applying CNN on infrared images of rigid PVC pipes used for sewers and comparing the results. The verified results showed that the AdaBoost method had the highest F-value (0.75) and accuracy among the ensemble learning methods. Furthermore, the artificial neural network was the second-highest performing method, with an accuracy of 0.72 and an F-value of 0.73.

In recent years, research on water leakage detection focusing on the application of machine learning methods and IoT technology using sensor or camera data was introduced [15–18]. Quantitative data often used include hydraulic physics variables such as the water pressure and flow in pipes. Acoustic data from sensors installed on pipes were also incorporated. In general, the purpose of using IoT communication technology is to monitor pipe networks. The machine learning methods adopted comprise feature extraction using PCA [19,20], ensemble learning [21,22], and CNN [23–25]. Some studies used deep learning techniques such as CNN; this method needs to be considered for developing leakage detection technology.

Hu et al. [26] classified various methods for detecting leakage locations in water distribution systems and classifying them into two categories: model- and data-based methods. They also reviewed leakage detection methods. They stated that the weakness of the model-based method was due to the lack of a calibrated hydraulic model used to distinguish water leakage. The discrimination results were also greatly influenced by model and measurement errors. The weakness of the data-based method was because it required a large amount of data to identify a water leakage, and the detection results were greatly influenced by data shortages, abnormal values, and noise. Therefore, the preference for model- or data-based methods depends on the amount of data obtained from the actual network and the difficulty of developing a hydraulic model of the network in question. Tina et al. [27] proposed a leakage detection method combining pipe flow rate

measurements using sensors and an Arduino system merged with IoT technology. The sensors were placed at the start and end points of the pipe, while the flow data obtained from the two were compared to detect leakage. This research verified leakage detection using the proposed method prototype. The results showed that, assuming no difference in flow between the start and end points, no leakage was detected.

Recent research on monitoring water distribution networks and leakage detection using IoT technology and hydraulic and deep learning model is important. Based on the literature review, our research focused on two aspects that were not adequately considered. First, we focused on leakage detection methods when acoustic data were used for analysis. In previous research, data such as changes in water pressure, pipe vibrations, or infrared images were used for analysis or training. However, research on the use of acoustic data to detect leakage is lacking. This method was considered suitable for continuous monitoring of leakage in pipelines, due to the easy acquisition of acoustic data, and the conventional process adopted by water management companies, namely the survey procedure relying solely on human hearing.

Second, there is a focus on the usefulness of deep learning methods in this context. This method is associated with the black box problem—the process of generating information that cannot be clearly understood. Therefore, research may be conducted without discerning the fundamental reasons behind the ability of deep learning to detect leakage. Ito et al. [3] explored the CNN model using a RP-CNN model, and reported that, at certain points, detection accuracy was below 80%. However, the causes of this low accuracy were not properly investigated.

The present research analyzed past failure cases, using PCA to reduce the dimensions of features based on frequency components and investigate the causes of inaccuracy. The distinctiveness of points with low accuracy was visualized through a sample plot diagram obtained from the principal component scores. This method was used to address the aforementioned problems, differentiating this study from previous research. Additionally, our research included results of blind tests conducted by leakage investigators using human hearing, particularly when evaluating statistical analysis and model accuracy. This increased the reliability of the results, providing original values not recorded in previous research.

2. Materials and Methods

2.1. Overview of Dataset

Acoustic data collection, focusing on water leakage sound and background noise in fields located in the Kanto region, Japan, was carried out using sensors. Each recording session lasted for 1 min to ensure consistent data collection across all scenarios. Additionally, the water leakage sound was recorded before carrying out repairs, and recording the background noise depended on reinstalling the sensors after repairs had been completed. Regarding background noise, other conditions remained the same except for the presence or absence of water leakage. When a leakage occurred, a location was selected—enabling the installation of sensors, such as gate valves, water control valves, or a fire hydrant, at the shortest distance. This ensured that the sound label did not only contain noise. Sensors A and B, installed at two locations closest to the leakage point, were used to collect both sounds. The sensors were strategically placed to measure the leakage distance accurately by comparing sound signal time delays and positioned away from pipe bends or branches to minimize sound distortions, ensuring clearer signals. Optimal placement provides a direct, unobstructed path to the leakage site, avoiding the frequency loss caused by pipe branching. The measurement distance from each sensor to the leakage point differed, and there may also have been branches or bends in the pipe. Despite there being only one

leakage point at each location, the sounds obtained from the two sensors differed. Leakage was detected using a correlation formula to compare the sound when it occurred and the background noise after repairs had been completed. The dataset focused on ductile iron pipe because this research aimed to conduct a basic analysis of the acoustic data recorded from such a pipe network.

Water leakage sound and background noise were recorded before and after repairs at the same location. The data about the existing conditions of the leakage location were the same. This resulted in a quality dataset for machine learning, perceived as a significant advantage. Furthermore, acoustic data, obtained at five leakage locations using 10 observation points, were used. When a leakage occurred at a particular location, the sound data were collected at two points: sensors A and B. Therefore, the acoustic data were symbolized in pairs as {1-A | 1-B}, . . . , {5-A | 5-B}, with a sampling frequency of 10,000 Hz. Frequency components greater than 5000 Hz (Nyquist frequency) could not be reproduced accurately due to aliasing effects, leading to exclusion from the data analysis. Information about 10 acoustic data points is given in Table 1, including leakage volume (L/min), measurement distance (m), sensor installation location, causes of leakage, sound pressure level (dB), water pressure (MPa), pipe diameter (mm), and soil cover (mm). The results of the blind test conducted by leakage investigators using the acoustic data are shown in Table 2. As dB values vary across frequencies in the waveform audio file, we calculated the average value of the data from 0 to 1500 Hz as the representative dB measurement for each acoustic data point, which is the same dataset used by the leakage investigator for the blind test.

Table 1. Detailed information on acoustic data.

| Point | Leakage Volume (L/min) | Measurement Distance (m) | Sensor Location | Cause of Leakage | Sound Pressure Level (dB) | Water Pressure (MPa) | Pipe Diameter (mm) | Soil Cover (mm) |
|-------|------------------------|--------------------------|-----------------|-----------------------------|---------------------------|----------------------|--------------------|-----------------|
| 1-A | 61.10 | 23.30 | gate valve | water faucet-bolt corrosion | 63.63 | 0.40 | 75 | 1250 |
| 1-B | | 21.90 | fire hydrant | | 64.45 | | | |
| 2-A | 34.35 | 113.00 | gate valve | water faucet-bolt corrosion | 72.27 | 0.35 | 150 | 1350 |
| 2-B | | 24.30 | gate valve | | 80.29 | | | |
| 3-A | 106.49 | 51.60 | gate valve | water faucet-corrosion | 72.64 | 0.35 | 100 | 1230 |
| 3-B | | 47.90 | fire hydrant | | 84.75 | | | |
| 4-A | 3.58 | 0.13 | gate valve | flange loose-bolt | 72.59 | 0.44 | 100 | 1200 |
| 4-B | | 38.07 | gate valve | | 78.02 | | | |
| 5-A | 93.25 | 13.70 | gate valve | water faucet-corrosion | 64.89 | 0.50 | 100 | 1220 |
| 5-B | | 44.80 | gate valve | | 63.48 | | | |

Table 2. Blind test results conducted by water leakage investigators.

| Point | Water Leak Sound | Background Noise |
|-------|---|--|
| 1-A | A high-pitched, resonant sound. Easy to determine as a water leak. | A general noise (buzzing). No sound of water leakage is heard. |
| 1-B | A distinctive high-pitched sound (koo). Easy to determine as a water leak. | Some noise, but no sound of water leak is heard. |
| 2-A | Difficult to distinguish, but a low resonant sound (rumble). Determined to be a water leak. | A general noise (rumble). No sound of water leakage is heard. |
| 2-B | A low-pitched sound of water leak. Easy to determine. | No sound of leaking can be heard. |

Table 2. Cont.

| Point | Water Leak Sound | Background Noise |
|-------|--|--|
| 3-A | A distinctive high-pitched and resonant sound. Easy to determine. | A general noise (rumble). No water leak sound is heard. |
| 3-B | Noise and a constant low resonance. Cannot be determined as the sound of a water leak. | A general noise (rumble). No sound of leaking water can be heard. |
| 4-A | A high-pitched, distinctive sound (goo). Easy to determine. | It sounds like running water. There are no other characteristic sounds of leakage. |
| 4-B | Noise and low-pitched sound. Cannot be determined as a water leak sound. | A high, constant sound (transformer sound). No sound of leakage can be heard. |
| 5-A | A distinctive high-pitched and resonant sound. Determined to be a water leak. | The sound of leakage (a continuous high-pitched, resonant sound) cannot be heard. |
| 5-B | Sound is faint but high-pitched and resonant. Determined to be a water leak. | A general noise (rumble). No sound of leaking water can be heard. |

2.2. Overview of Water Leakage Determination Based on an RP-CNN Model

An RP-CNN model was adopted to determine leakage, using a CNN, a type of deep learning method. An RP is a visualization tool used to convert the one-dimensional data obtained from sensors into two-dimensional data. A CNN model can utilize an RP to identify unique patterns within acoustic data, enabling the separation of leakage signals from complex background noise. The RP patterns for water leakage sound typically exhibit structured, precise, honeycomb-like shapes. In contrast, RP patterns for background noise appear more scattered and irregular, lacking distinct patterns. Leakage sound demonstrates more deterministic and periodic characteristics compared to background noise. An interval of 0.008 and size of 64 were used as parameters to convert time-series data into RP. This was also applied using the representation of recorded water leakage sound and background noise (RP) data for learning and assessment (Figure 1). Leakage was distinguished by using the deterministic nature of the difference between the leak sound and background noise [1]. The discrimination accuracy of the RP-CNN model was previously verified [2,3]; it could distinguish between leakage sound and background noise with an accuracy rate of approximately 80% in some locations.

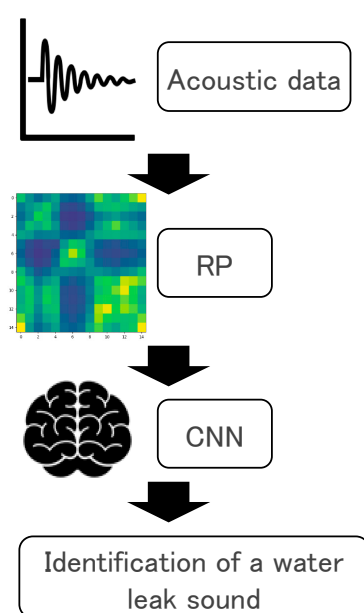


Figure 1. Flowchart of water leakage determination using the RP-CNN model.

Learning and assessment datasets are crucial when using a machine learning method. Previous research [3] focused on evaluating the generalization performance using learning data from several locations (besides assessment data) in a 9-point model (Figure 2). The present research concentrated on investigating the causes of lower accuracy (points 3-B and 4-B) and the improvement process. In order to verify the effectiveness of feature amplification and the use of band-stop filters to eliminate AC frequency interference (pre-processing), a 10-point model was adopted with the assessment data applied to the learning process. Therefore, the difficulty in determining leakage sound and background noise observed at various locations, including the possibility of assessment errors, was evaluated using a general model.

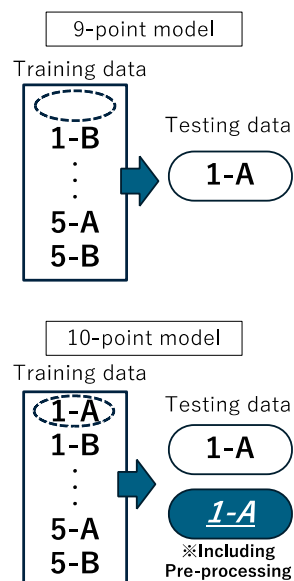


Figure 2. Learning and assessment data for 9- and 10-point models.

3. Results and Discussion

3.1. PCA Application Method

Principal component analysis is a statistical method that reduces multidimensional data to a low-dimensional space without losing important information. It is often used for dimension reduction and visualization in data evaluation. According to the Scikit-Learn Data Analysis Implementation Handbook (Shuwa System), the main purposes of dimensionality reduction are data compression and visualization. This is achieved by algorithms such as PCA, feature selection, and non-negative matrix factorization. Additionally, PCA was previously used to investigate the causes of low accuracy at several locations [3,28]. Dimension reduction and visualization comprised two stages.

Stage 1: Application of Fast Fourier Transform (FFT) (data dimension reduction)

Based on previous research, the effective frequency range for detecting leakage in ductile iron pipe is less than 1500 Hz [29]. Our research focused on 153 frequency components of approximately 1500 Hz obtained from FFTs. For data grouping, the frequency components were divided into 15 categories (<100 Hz, <200 Hz, . . . , <1400 Hz, <1500 Hz), with each represented by a mean value. In this process, the data were converted into 15 dimensions. The implementation of this method ensured that the number of variables ($n = 15$) used in the PCA did not exceed the number of samples ($n = 20$).

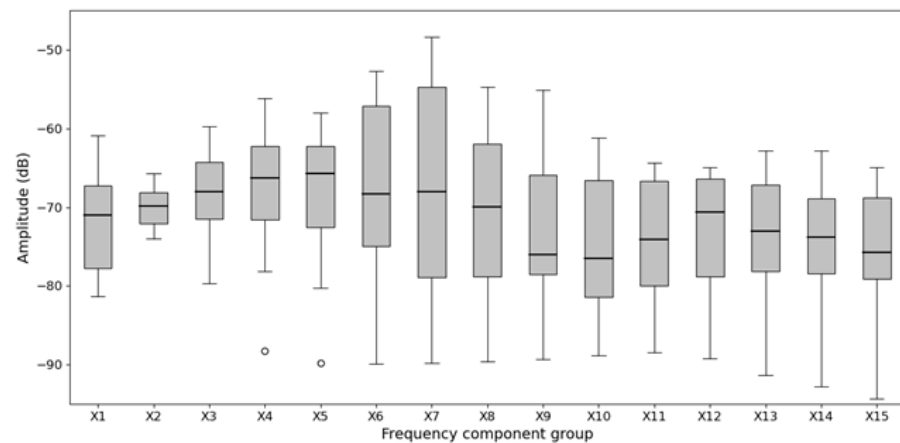
Stage 2: Application of PCA (dimension reduction and visualization)

Considering the 15-dimensional data (FFT), PCA was used to obtain the first (PC1) and second (PC2) principal components. We then positioned the samples according to the PC1

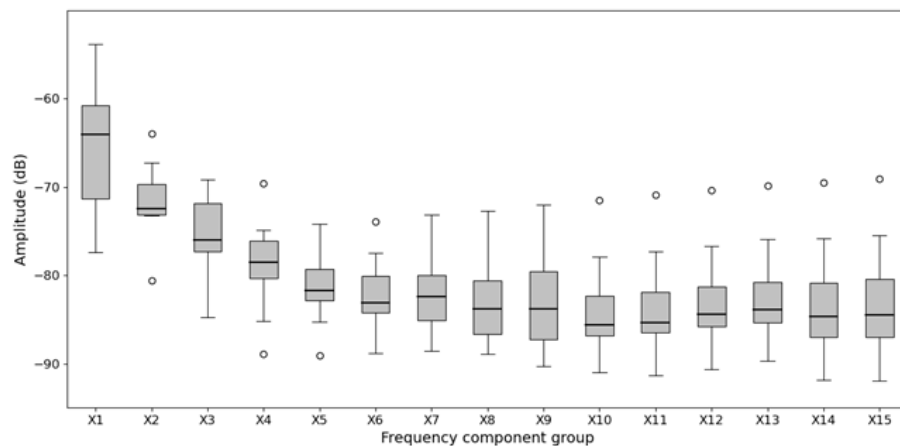
and PC2 scores to classify locations with (10 locations) and without leakage (10 locations). In the PCA stage, the data were also re-standardized by centralizing (making the mean value 0) and scaling (making the standard deviation 1). This analysis was performed using version 4.3.2 of Windows software.

3.2. Sample Position Results Based on PCA Scores

A box plot diagram was generated using 15-dimensional data to distinguish between the sound of water leakage and background noise. The median value for water leakage reached a peak within the frequency range of variables X4–X6. Meanwhile, background noise reached a peak at variable X1, gradually decreasing in the higher frequency range (Figure 3). This implied that the average characteristic pattern between the two differed.



(a) Water leakage sound



(b) Background noise

Figure 3. Box plot of acoustic data converted into 15 dimensions.

The results of the sample position, in accordance with the principal component scores, are shown in Figure 4. The contributions of PC1 and PC2 were 0.696 and 0.150, respectively. The focus on leakage sound, denoted by ● in Figure 4, implied that it was mostly distributed in the positive direction on PC1 (horizontal axis). However, the background noise, denoted by ▲, was mostly distributed in the negative direction on PC1 (horizontal axis). The leakage sound in samples 3-B and 4-B was not located in the zone where the other points were distributed but projected into the area occupied by the background noise. Compared to the results of the blind test (Table 2), the sound in samples 3-B and 4-B was consistently disregarded. The low accuracy in samples 3-B and 4-B in the RP-CNN model was caused by

low recall and specificity outcomes for leakage sound and background noise, respectively. This suggested that there may be a problem with the acoustic data of leakage sound (recall). The acquired sound characteristics were distorted by certain influences resembling background noise. This made assessment difficult for both the RP-CNN model and the investigators. Additionally, both leakage sound and background noise from the same location were detected on the right and left sides of the PC1 axis, respectively. In sample 4-B with low accuracy, the left–right relationship on the PC1 axis was maintained, but in 3-B, leakage sound and background noise were on the left and right sides, respectively. Aside from the left–right inversion, a short distance between the leakage sound and background noise was characteristic of sample 3-B in contrast to other samples.

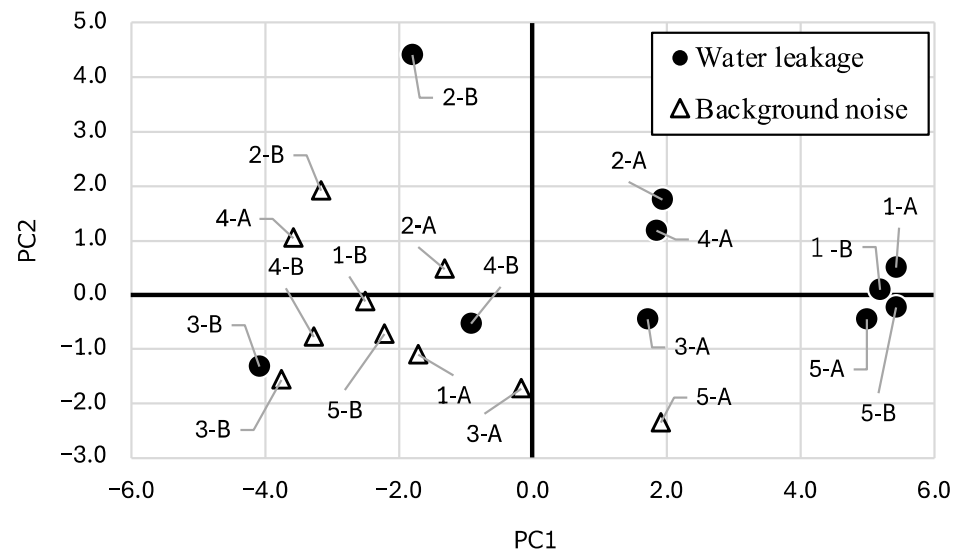


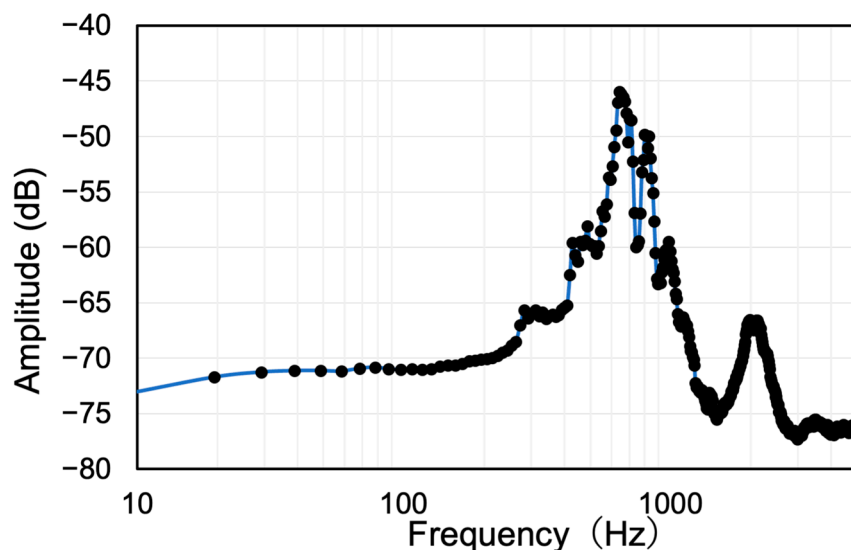
Figure 4. Positioning results based on principal component scores.

3.3. Pre-Processing for Emphasizing Leakage Sounds and Eliminating Background Noise

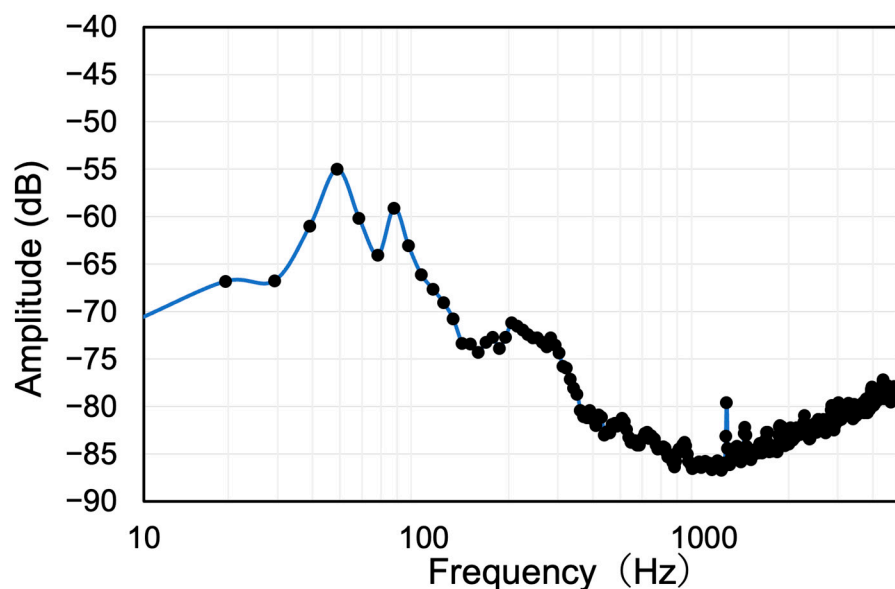
Section 3.2 showed that a possible cause of the low accuracy at points 3-B and 4-B was interference in the acoustic data. Recording and transmission were carried out using acoustics by altering the frequency characteristics while considering distortion and noise. An acoustic device (an equalizer) was used to improve the sound quality and reduce certain frequencies, thereby overcoming the problem of noise, howling, or excessive echo.

A water leakage sound is similar to background noise because its unique characteristics do not fully reach the recording point (sensor). This causes the characteristics that should be present in leakage sound data to be weakened. In such cases, it becomes necessary to focus on emphasizing leakage sound characteristics. Therefore, to improve the accuracy of sound detection on data with such problems, a pre-processing method that concentrates or reduces certain frequency bands is considered an effective countermeasure.

A typical example of the FFT spectrum comparing leakage sound and the background noise at point 1-B is shown in Figure 5. This showed that the sound spectrum had a peak in the relatively high-frequency region, greater than 500 Hz. For the background noise, the frequency region greater than 500 Hz showed a flat pattern without peaks. This pattern was observed at other locations, including 1-B. The box plot of data transformed into 15 dimensions shows that leakage sound had a peak of approximately 500 Hz (Figure 3).



(a) Water leakage sound



(b) Background noise

Figure 5. FFT spectrum of point 1-B.

Considering this result, further analysis assumed the frequency region that characterized leakage sound was within 500–600 Hz, leading to the application of an amplification process. However, not all frequency components within 500–600 Hz were amplified. Amplification was performed only when the absolute value of the Fourier transform result, $|X(k)|$, exceeded 5.5 (with k as the frequency value), to reduce the influence on background noise. Additionally, for sound to reach the ideal conditions, it is important to increase necessary sound and reduce unnecessary sound. A reduction can also be performed to eliminate weak noise, aside from amplifying certain frequencies. Therefore, frequencies with $|X(k)| > 0.9$ were also reduced in this process.

In the present study, we also concentrated on the eradication of sounds similar to water leaks (pseudo-leak sounds), such as transformer sounds, by adopting a method of eliminating 50 and 60 Hz frequency components, including respective harmonics, using a

band-stop filter. This also aimed to reduce errors in identifying the acoustic data affected by transformer sound, thereby increasing specificity.

Figure 6 shows an example of changes in RP of leakage sound at point 4-B (from 2000 to 2002) after the amplification process, where a honeycomb pattern was observed. These results implied that, by amplifying the frequency components of 500–600 Hz, the typical leakage sound at point 4-B was successfully acquired.

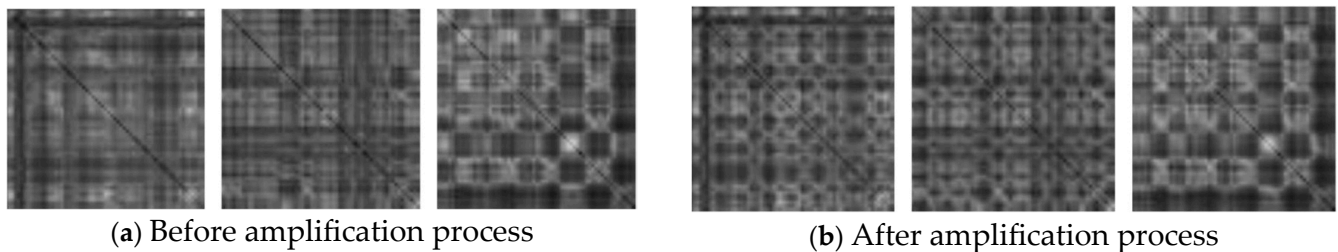


Figure 6. Changes in RP due to amplification process of point 4-B (RP number 2000 to 2002).

The dimension reduction and data visualization methods with PCA used in Section 3.2 were applied to verify the effect of pre-processing. The outcome before and after the application of the process was compared (Figure 7). Adjustments were made by amplifying and reducing frequency components with $|X(k)| > 5.5$ and $|X(k)| < 0.9$, respectively. Meanwhile, this amplification and reduction improved leakage sound and background noise. Similar peak changes were obtained when assuming that the background noise within the frequency range of 500–600 Hz had the same characteristics as leakage sound. The slope of the 15-dimensional data implies that these frequencies did not show the changes observed in leakage sound. Therefore, it can be considered appropriate to assume that the typical region of leakage sound was within 500–600 Hz, as well as the decision to target this frequency range for the amplification process.

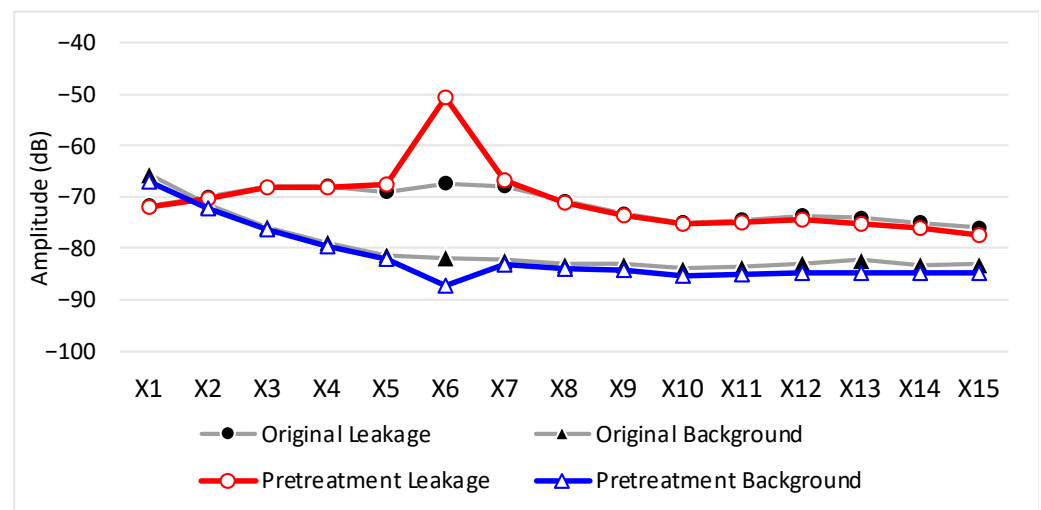


Figure 7. Results of applying the proposed method (15-dimensional data).

3.4. Water Leakage Determination Test Using the RP-CNN Model

This study examined the effect of the proposed pre-processing: (1) strengthening the frequency components within 500–600 Hz only for $|X(k)| > 5.5$ (prominence in the characteristics of typical leakage sound); (2) removing frequency components with $|X(k)| < 0.9$ (weak noise reduction); and (3) using a band-stop filter to eliminate the 50 Hz frequency and respective harmonics (AC noise removal). These three pre-processing methods were verified in the present study. Specifically, two types of datasets (pre-processed and not

pre-processed) were acquired, and the accuracy of the RP-CNN model was determined after usage. The testing data differed from the training data used to build the model. The parameters of the RP-CNN model were as follows: interval 0.016 s, size 64, LPF 4000 Hz, and batch size 16. In terms of determining the number of epochs, the model with the highest accuracy on the testing data was adopted (epoch = 10). It is generally recommended to treat validation data and training data separately. Validation data were used to adjust hyperparameters, such as batch size, when building the model.

The results after applying the RP-CNN model on the three methods are shown in Table 3. Initially, the results for without pre-processing showed that the recall for 3-B and 4-B was 0%. Furthermore, for 3-B and 4-B, the RP-CNN model considered leakage sound as background noise, resulting in a recall of 0%. These results were in accordance with previous research [3], as demonstrated in Table 4, and the positioning performed using principal component scores. However, the results with pre-processing showed that the recall for 3-B and 4-B increased to 64.4% and 81.4%, respectively. This suggested improvement due to pre-processing.

Table 3. Results of applying the RP-CNN model to the assessment data.

| (a) Non-Pre-Processed Data | | | | |
|-----------------------------------|-------|--------------|--------|-------------|
| Point | Epoch | Accuracy (%) | | |
| | | BA | Recall | Specificity |
| 1-A | 10 | 99.3 | 99.9 | 98.7 |
| 1-B | | 99.8 | 100.0 | 99.6 |
| 2-A | | 94.9 | 95.4 | 94.3 |
| 2-B | | 94.6 | 97.7 | 91.5 |
| 3-A | | 98.4 | 99.3 | 97.5 |
| 3-B | | 49.4 | 0.0 | 98.8 |
| 4-A | | 98.1 | 99.6 | 96.6 |
| 4-B | | 46.8 | 0.0 | 93.6 |
| 5-A | | 99.6 | 99.3 | 99.9 |
| 5-B | | 98.6 | 97.4 | 99.8 |
| (b) Pre-Processed Data | | | | |
| Point | Epoch | Accuracy (%) | | |
| | | BA | Recall | Specificity |
| 1-A | 10 | 97.8 | 99.9 | 95.6 |
| 1-B | | 89.4 | 100.0 | 78.8 |
| 2-A | | 97.9 | 100.0 | 95.8 |
| 2-B | | 95.8 | 100.0 | 91.6 |
| 3-A | | 99.5 | 100.0 | 98.9 |
| 3-B | | 81.8 | 64.4 | 99.2 |
| 4-A | | 95.9 | 100.0 | 91.8 |
| 4-B | | 88.7 | 81.4 | 95.9 |
| 5-A | | 99.6 | 100.0 | 99.1 |
| 5-B | | 99.7 | 100.0 | 99.4 |

Table 4. Comparison of accuracy between previous and current research.

| Point | Previous Research | | | Current Research | | |
|-------|-------------------|--------|-------------|------------------|--------|-------------|
| | Accuracy (%) | | | | | |
| | BA | Recall | Specificity | BA | Recall | Specificity |
| 3-B | 62.7 | 58.9 | 64.8 | 81.8 | 64.4 | 99.2 |
| 4-B | 75.3 | 66.1 | 84.4 | 88.7 | 81.4 | 95.9 |

Previous research [3] combined a 9-point model and noise reduction methods.

The visual comparison of RP data also highlighted pattern changes before and after pre-processing at points 3-B and 4-B (Figure 8). The visual results before pre-processing exhibited irregular and blurred patterns, making it challenging for the model to identify the characteristics of leakage sounds obscured by background noise. Conversely, a clear and structured honeycomb pattern (a distinctive characteristic of water leakage sounds) was evident after applying pre-processing at point 4-B. This indicated that the method successfully reduced noise and enhanced the unique features of the leakage sound. However, after pre-processing, the RP visualization at point 3-B shows a straight-line pattern with perpendicular hyperbolic shapes resembling pseudo-leakage sound patterns.

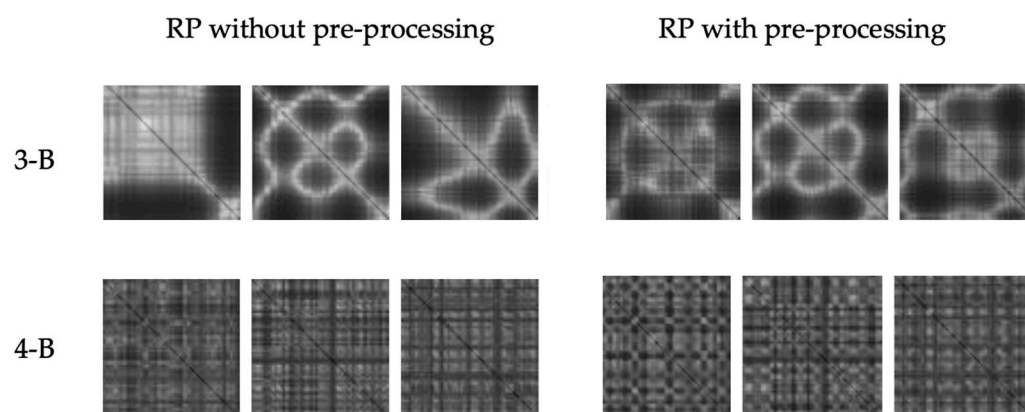


Figure 8. Changes in RP before and after pre-processing of points 3-B and 4-B.

Furthermore, the effectiveness of the proposed method in this study was validated by the results of a confusion matrix plot, which consists of four classifications: true positive (TP), false negative (FN), false positive (FP), and true negative (TN). The results showed that there were no TP instances without pre-processing, as all leakage sounds were misclassified as no leakage (Figure 9). When pre-processing was applied, there was a significant improvement, with TP increasing by 64% and achieving a higher overall balanced accuracy at point 3-B. Additionally, the TP at point 4-B increased significantly to 81.4%. This demonstrated that pre-processing enhances the model's ability to detect leakage signals while accurately reducing FN instances.

These results demonstrated that applying pre-processing significantly improves the accuracy of leakage detection, as evidenced by the increase in TP rates at points 3-B and 4-B. This highlighted the effectiveness of the proposed method in separating leakage signals from background noise. These findings aligned with advancements in IoT-based water monitoring systems, which have shown the potential to enhance detection accuracy through real-time data processing and smart technologies [30]. The integration of such systems can further support predictive analysis and proactive maintenance in water networks [30].

Although the increase in recall accuracy was confirmed in all cases, a negative aspect (adverse impact of pre-processing, i.e., a decrease in specificity) was observed in five out of every ten cases. This issue was observed in 1-B, where specificity decreased by more than 20%. Despite the improved recall for the expected results, the problem of specificity remained. Recall for 3-B was lower than for other points and the limitations proven by the pre-processing effect. The PCA showed that 3-B tended to exhibit unique acoustic data and a different pattern to the other points, with the leakage sound and background noise on the left and right sides of the PC1 axis, respectively. Further data collection and accumulation are required, irrespective of whether the data are unique or there are similar cases. This research requires further in-depth observation, considering implementation in the real world.

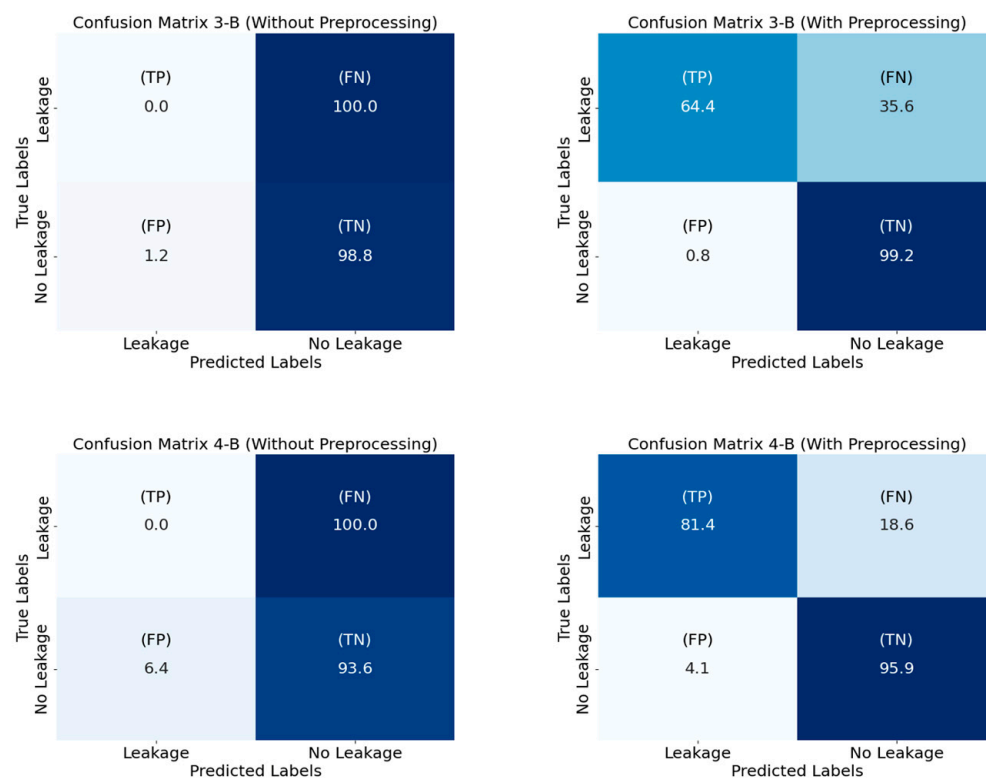


Figure 9. Comparison of confusion matrix for points 3-B and 4-B.

4. Conclusions

This study investigated the causes of inaccuracies in leakage determination and an RP-CNN was used to gain insights to improve the generalization of the model. A basic analysis of leakage sound and background noise was conducted in water pipes and visualized acoustic data were assessed by using the FFT and RP. Additionally, a pre-processing method was proposed for acoustic data, including RP pattern changes. The accuracy of leakage detection using the RP-CNN model was studied. The results of this research are as follows:

- (1) The frequency components obtained from the FFT (up to 1500 Hz) showed that the data obtained were converted into 15 dimensions, leading to PCA. The results from sample classification using the PC1 and PC2 scores showed that leakage sound at points 3-B and 4-B was in an area with a lot of background noise. This was consistent with the blind test conducted by leakage investigators, in which the sound at points 3-B and 4-B could not be identified.
- (2) Based on the differences in the FFT spectrum, an amplification process was applied within the frequency range of 500–600 Hz for water leakage sound. After its application, a new honeycomb pattern was found in RP at the problematic location. This showed that the amplification process within this range effectively focused on the characteristics of leakage sound.
- (3) To test the effectiveness of the proposed pre-processing method, two datasets were obtained (with and without pre-processing), and the accuracy of the RP-CNN model was evaluated. The results without pre-processing showed a recall of 0% for points 3-B and 4-B, while after pre-processing, this increased to 64.4% and 81.4%, respectively. This implied an improvement in recall with the application of pre-processing.

The present research focused on the frequency components of 500–600 Hz. The amplification process confirmed a honeycomb pattern in leakage sound RP at the problematic location. However, the location of frequency components that best reflected the characteristics of leakage sound was not completely clear. Future sensitivity analyses should determine the effect of changes in the amplified frequency components while drawing RP and identify those containing the most characteristics of leakage sound. This is crucial for exploring more effective ways of applying the proposed pre-processing method.

Furthermore, although the current findings and methodology provide a strong foundation for water leakage detection, several challenges remain to be addressed to enhance practical implementation and data accuracy. One recommended strategy is the application of map planning for existing pipeline conditions. A comprehensive understanding of pipeline layouts, including branches and curves, allows for strategic sensor placement, minimizing acoustic distortions and improving detection accuracy. Map planning not only supports efficient planning and reduces operational costs but also facilitates the integration of future technologies for predictive analysis. This approach strengthens the calibration of models such as RP-CNN, resulting in more reliable predictions. Analyzing the interplay between optimal frequency components, effective pre-processing, and sensor placement based on map planning creates a pathway for achieving more efficient and precise leakage detection in real-world applications.

Author Contributions: Conceptualization, M.A.C., T.S. and Y.A.; methodology, M.A.C. and Y.A.; software, T.S.; validation, M.A.C. and Y.A.; formal analysis, M.A.C. and T.S.; investigation, M.A.C.; resources, M.A.C. and X.D.; data curation, M.A.C. and T.S.; writing—original draft preparation, M.A.C. and Y.A.; writing—review and editing, M.A.C.; visualization, M.A.C.; supervision, Y.A., T.K. and A.K.; project administration, Y.A.; funding acquisition, Y.A. All authors have read and agreed to the published version of the manuscript.

Funding: This research was funded by JSPS KAKENHI (grant number JP22K04271) and the Tokyo Metropolitan Government Advanced Research Program (R4-2).

Data Availability Statement: The original contributions presented in this study are included in the article. Further inquiries can be directed to the corresponding author.

Acknowledgments: The first author is grateful to the Tokyo Human Resources Fund (THRF) for financial support during his graduate research.

Conflicts of Interest: The authors declare no conflicts of interest.

Abbreviations

| | |
|-------|--|
| SIP | strategic innovation promotion program |
| RP | recurrence plot |
| CNN | convolutional neural network |
| BA | balanced accuracy |
| PCA | principal component analysis |
| TTBTs | transient test-based techniques |
| FFT | fast Fourier transform |

References

1. Nam, Y.; Arai, Y.; Kunizane, T.; Koizumi, A. Developing of Water Leakage Discrimination Model using Recurrence Plot and Convolutional Neural Network. *J. Jpn. Soc. Civ. Eng. Ser. G* **2020**, *76*, II 273–II 284. [[CrossRef](#)]
2. Shimada, M.; Arai, Y.; Kunizane, T.; Koizumi, A. Evaluation of the Water Leakage Detection Model by Training Multiple Water Leakage Sounds. *J. Jpn. Soc. Civ. Eng. Ser. G* **2022**, *78*, II 141–II 152. [[CrossRef](#)] [[PubMed](#)]

3. Ito, K.; Arai, Y.; Caronge, M.A.; Kunizane, T.; Koizumi, A. Improving the Generalization Performance of Water Leakage Detection Model by Noise Reduction Using Pseudo Sounds. *J. Jpn. Soc. Civ. Eng.* **2023**, *79*, 23–26009. [[CrossRef](#)]
4. Asada, Y.; Kimura, M.; Azechi, I.; Iida, T. Leak Detection Using Transient Pressure Waves in Pipelines with Multiple Leaks and Characteristic Structure. *J. Jpn. Soc. Civ. Eng. Ser. B1* **2020**, *76*, I 937–I 942. [[CrossRef](#)] [[PubMed](#)]
5. Meniconi, S.; Capponi, C.; Frisinghelli, M.; Brunone, B. Leak Detection in a Real Transmission Main Through Transient Tests: Deeds and Misdeeds. *Water Resour. Res.* **2021**, *57*, e2020WR027838. [[CrossRef](#)]
6. Duan, H.F.; Lee, P.J.; Ghidaoui, M.S.; Tuck, J. Transient wave blockage interaction and extended blockage detection in elastic water pipelines. *J. Fluids Struct.* **2014**, *46*, 2–16. [[CrossRef](#)]
7. Duan, H.F.; Lee, P.J. Transient-based frequency domain method for dead-end side branch detection in reservoir-pipeline-valve system. *J. Hydraul. Eng.* **2016**, *142*. [[CrossRef](#)]
8. Ayati, A.H.; Haghighi, A.; Lee, P. Statistical Review of Major Standpoints in Hydraulic Transient-Based Leak Detection. *J. Hydraul. Struct.* **2019**, *5*, 1–26. [[CrossRef](#)]
9. Ferrante, M.; Brunone, B. Leak detection in branched pipe systems coupling wavelet analysis and a Lagrangian model. *Aqua* **2009**, *58*, 95–106. [[CrossRef](#)]
10. Haghighi, A.; Covas, D.; Ramos, H. Direct backward transient analysis for leak detection in pressurized pipelines: From theory to real application. *Aqua* **2012**, *61*, 189–200. [[CrossRef](#)]
11. Duan, H.F. Transient frequency response-based leak detection in water supply pipeline systems with branched and looped junctions. *J. Hydroinform.* **2017**, *19*, 17–30. [[CrossRef](#)]
12. Kim, S.H.; Zecchin, A.; Choi, L. Diagnosis of a Pipeline System for Transient Flow in Low Reynolds Number with Impedance Method. *J. Hydraul. Eng.* **2014**, *140*. [[CrossRef](#)]
13. Kim, S.H. Multiple Leak Detection Algorithm for Pipe Network. *Mech. Syst. Signal Process.* **2020**, *139*, 106645. [[CrossRef](#)]
14. Shirahata, H.; Numadu, R. Application of Machine Learning for Detection of Leakage in Drain Pipes by Infrared Camera. *J. AI Data Sci.* **2022**, *3*, 223–230. [[CrossRef](#)]
15. Gama-Moreno, L.A.; Corralejo, A.; Molina, A.R.; Rangel-Torres, J.A.; Hernandez, C.M.; Juarez, M.A. A Design of a Water Tanks Monitoring System Based on Mobile Devices. In Proceedings of the 2016 International Conference on Mechatronics, Electronics and Automotive Engineering (ICMEAE), Cuernavaca, Mexico, 22–25 November 2016; pp. 133–138. [[CrossRef](#)]
16. Chan, T.K.; Chin, C.S.; Zhong, X. Review of Current Technologies and Proposed Intelligent Methodologies for Water Distributed Network Leakage Detection. *IEEE Access* **2018**, *6*, 78846–78867. [[CrossRef](#)]
17. Guatam, J.; Chakrabarti, A.; Agarwal, S.; Singh, A.; Gupta, S.; Singh, J. Monitoring and Forecasting Water Consumption and Detecting Leakage Using an IoT System. *J. Water Supply* **2020**, *20*, 1103–1113. [[CrossRef](#)]
18. Ayamga, M.A. An IoT-Based Water Leakage Detection and Localization System. *Asian J. Res. Comput. Sci.* **2024**, *17*, 1–14. [[CrossRef](#)]
19. Zhuo, M.; Zhang, Q.; Liu, Y.; Sun, X.; Cai, Y.; Pan, H. An Integration Method Using Kernel Principal Component Analysis and Cascade Support Vector Data Description for Pipeline Leak Detection with Multiple Operating Modes. *Processes* **2019**, *7*, 648–665. [[CrossRef](#)]
20. Hashim, H.; Ryan, P.; Clifford, E. A Statistically Based Fault Detection and Diagnosis Approach for Non-residential Building Water Distribution Systems. *Adv. Eng. Inform.* **2020**, *46*, 101187. [[CrossRef](#)]
21. Ravichandran, T.; Gavahi, K.; Ponnambalam, K.; Burtea, V.; Mousavi, S.J. Ensemble-based Machine Learning Approach for Improved Leak Detection in Water Mains. *J. Hydroinform.* **2021**, *23*, 307–323. [[CrossRef](#)]
22. Shi, M.; Deng, L.; Yang, B.; Qin, L.; Gu, L. Research on Internal Leakage Detection of the Ball Valves Based on Stacking Ensemble Learning. *Meas. Sci. Technol.* **2024**, *35*, 095109. [[CrossRef](#)]
23. Kang, J.; Park, Y.J.; Lee, J.; Wang, S.H.; Eom, D.S. Novel Leakage Detection by Ensemble CNN-SVM and Graph-based Localization in Water Distribution Systems. *IEEE Trans. Ind. Electron.* **2018**, *65*, 4279–4289. [[CrossRef](#)]
24. Javadiha, M.; Blesa, J.; Soldevila, A.; Puig, V. Leak Localization in Water Distribution Networks Using Deep Learning. In Proceedings of the 6th International Conference on Control, Decision and Information Technologies, Paris, France, 23–26 April 2019; pp. 1426–1431. [[CrossRef](#)]
25. Cody, R.A.; Tolson, B.A.; Orchard, J. Detecting Leaks in Water Distribution Pipes Using a Deep Autoencoder and Hydroacoustic Spectrograms. *J. Comput. Civ. Eng.* **2020**, *34*, 1–8. [[CrossRef](#)]
26. Hu, Z.; Chen, B.; Chen, W.; Tan, D.; Shen, D. Review of Model-based and Data-driven Approaches for Leak Detection and Location in Water Distribution Systems. *Water Supply* **2021**, *21*, 3282–3306. [[CrossRef](#)]
27. Tina, J.S.; Kateule, B.B.; Luwemba, G.W. Water Leakage Detection System Using Arduino. *Eur. J. Inf. Technol. Comput. Sci.* **2022**, *2*, 1–4. [[CrossRef](#)]
28. Kottegoda, N.T.; Rosso, R. *Statistics, Probability and Reliability for Civil and Environmental Engineers*; McGraw-Hill International Editions, Civil Engineering Series: Singapore, 1998; pp. 388–393.

29. Kawamura, W.; Arai, Y.; Koizumi, A.; Inakazu, T.; Yokokawa, K.; Kaji, K.; Suzuki, K.; Ariyoshi, H.; Moriyama, S. An Analysis of Pipeline Sensing Data Use for Detecting Water Leakage. *J. Jpn. Soc. Civ. Eng. Ser. G* **2016**, *72*, 187–194. [[CrossRef](#)]
30. Ullah, N.; Siddique, M.F.; Ullah, S.; Ahmad, Z.; Kim, J.M. Pipeline Leak Detection System for a Smart City: Leveraging Acoustic Emission Sensing and Sequential Deep Learning. *Smart Cities* **2024**, *7*, 2318–2338. [[CrossRef](#)]

Disclaimer/Publisher’s Note: The statements, opinions and data contained in all publications are solely those of the individual author(s) and contributor(s) and not of MDPI and/or the editor(s). MDPI and/or the editor(s) disclaim responsibility for any injury to people or property resulting from any ideas, methods, instructions or products referred to in the content.